Epigenetic cell memory: digital or analog?*

Simone Bruno[1,2] and Domitilla Del Vecchio[2]

***Abstract*— Epigenetic cell memory is the property enabling multicellular organisms to keep distinct cell types despite sharing the same genotype. DNA methylation and histone modifications play a crucial role in maintaining the long-term memory of gene expression patterns specific to each cell type. Experimental results in semi-synthetic genetic systems show that these modifications silence and reactivate genes in an "all or none" manner, suggesting digital epigenetic memory (only extremal gene expression levels have long-term memory). However, in recent years, continuous and graded variations of gene expression levels have been identified across multiple cell types. In this study, we introduce and analyze a mathematical model including both histone modifications and DNA methylation to demonstrate that the experimentally observed probability distributions of gene expression level, used to support digital memory hypothesis, are also compatible with analog memory hypothesis (cells can maintain any initially set gene expression level). Our study shows that intrinsic noise combined with an ultrasensitive response between the level of DNA methylation writer DNMT3A and DNA methylation grade at a gene causes the potential ambiguity. The model can then help design key experiments to conduct in order to distinguish between digital and analog memory, thereby offering a tool for interrogating the very essence of epigenetic cell memory.**

I. Introduction

Epigenetic cell memory (ECM) is the property of multicellular organisms to maintain different phenotypes despite sharing a common genetic sequence. This property is primarily influenced by the compaction of DNA structure (known as the chromatin state) [1], [2], regulated by epigenetic modifications to DNA and histones [1], [3]. More precisely, DNA methylation has been considered the essence of long-term memory, as it can persist through subsequent cell divisions by the action of enzymes that replicate the methylation pattern from the parental DNA strand onto the newly synthesized DNA strand during DNA replication [4].

In the past, experimental results suggested a genome-wide distribution of DNA methylation primarily concentrated at the extremal levels [5]–[7]. More recently, studies such as [8] support this notion, showing that chromatin modifiers transiently recruited to a gene influence the fraction of cells that are silenced or active, rather than directly affecting the gene expression level. Overall, these experimental results support the hypothesis of digital epigenetic cell memory (cells can stably maintain only silenced or active gene expression levels). However, in the past years, graded variations in gene expression levels have been observed across various cell types, such as the ones forming the mouse isocortex and hippocampus [9]. This suggests that cells must have a mechanism enabling them to maintain their specific gene expression level and associated identity.

Here, we explore how long-term memory of intermediate gene expression levels can be achieved and how chromatin modifications affect this process. Our goal is to demonstrate that the experimentally observed probability distributions of gene expression level, used to support digital memory hypothesis, are also compatible with analog memory hypothesis (cells can maintain any initially set gene expression level). To this end, we first introduce a mathematical model combining histone modifications and DNA methylation. We then exploit Gillespie's Stochastic Simulation Algorithm [10] to understand how system's parameters qualitatively affect gene expression memory. Furthermore, we derive a reduced model recapitulating the mechanisms behind analog memory and use it to determine how experimental results may be compatible with analog memory.

The paper is structured as follows: in Sections II and III we describe the models of chromatin modification circuit and gene expression, in Sections IV and V we describe the stochastic analysis conducted to determine how system's parameters affect gene expression memory, and in Section VI we present concluding remarks.

II. Chromatin modification circuit model

In this section, we briefly describe the chromatin modification circuit considered in our study, developed starting from the one in [11] (see [11] for a more detailed description). The chromatin modifications considered are H3K9 methylation (H3K9me3), H3K4 methylation (H3K4me3), and DNA methylation. In terms of species, the model includes unmodified nucleosome (D), nucleosome with H3K4me3 ($\mathrm{D^A}$), with DNA methylation, ($\mathrm{D_1^R}$), with H3K9me3 ($\mathrm{D_2^R}$), or with both H3K9me3 and DNA methylation ($\mathrm{D_{12}^R}$). The reaction model can be represented by the circuit diagram shown in Fig. 1(a), with

*This work was supported by NSF Collaborative Research grant MCB-2027949.

[1]Department of Data Science, Dana-Farber Cancer Institute, Boston, MA, 02115, USA.

[2]Department of Mechanical Engineering, Massachusetts Institute of Technology, Cambridge, MA, 02139, USA.

Emails: sbruno@ds.dfci.harvard.edu, ddv@mit.edu

the corresponding reactions provided in Table I. More precisely, writer enzymes can *de novo establish* chromatin marks and histone modifications can recruit these enzymes to establish the same modification on nearby modifiable nucleosomes (*auto-catalysis*) [1], [12], [13]. Furthermore, through *cross-catalysis*, DNA methylation and repressive histone modification enhance each other by recruiting each other's writer enzymes [14]. Eventually, these modifications are removed through dilution during DNA replication or by the action of eraser enzymes (*basal erasure*). Finally, erasers of activating modifications can be recruited by repressive modifications, and *viceversa* (*recruited erasure*) [3], [15]–[17].

Let us now introduced the corresponding ordinary differential equation (ODE) model in terms of $\bar{D}^A = n^A/\mathrm{D_{tot}}$, $\bar{D}_1^R = n_{D_1^R}/\mathrm{D_{tot}}$, $\bar{D}_2^R = n_{D_2^R}/\mathrm{D_{tot}}$, $\bar{D}_{12}^R = n_{D_{12}^R}/\mathrm{D_{tot}}$ and $\bar{D} = n_D/\mathrm{D_{tot}}$, with $\mathrm{D_{tot}}$ representing the total number of nucleosomes in the gene, and n^A, n_1^R, n_2^R, n_{12}^R, and n^D denoting the amount of $\mathrm{D^A}, \mathrm{D_1^R}, \mathrm{D_2^R}, \mathrm{D_{12}^R}, \mathrm{D}$. It is possible to do this by assuming $\mathrm{D_{tot}}$ large enough to consider $\bar{D}^A$, $\bar{D}_1^R$, $\bar{D}_2^R$, $\bar{D}_{12}^R$ and $\bar{D}$ real numbers. Now, let us introduce $D_{tot} = \mathrm{D_{tot}}/\Omega$, with Ω denoting the reaction volume, and the normalized inputs: $u_{i0}^R = k_{W0}^i/k_M^A D_{tot}$, $u_i^R = k_W^i/(k_M^A D_{tot})$, $u_0^A = k_{W0}^A/(k_M^A D_{tot})$, and $u^A = k_W^A/(k_M^A D_{tot})$, with $i = 1, 2$. Additionally, let

$$\alpha = k_M/k_M^A, \;\; \alpha' = k_M'/k_M^A, \;\; \bar{\alpha} = \bar{k}_M/k_M^A. \tag{1}$$

The parameter α is the non-dimensional rate constant associated with auto-catalysis and $\bar{\alpha}$, α' are the ones associated with cross-catalysis. Finally, let

$$\varepsilon = \frac{\delta + \bar{k}_E^A}{k_M^A D_{tot}}, \;\; \varepsilon' = \frac{k_E^A}{k_M^A}, \;\; \mu' = \frac{k_T'^*}{k_E^A}, \;\; \mu = \frac{k_E^R}{k_E^A}, \tag{2}$$

with $\beta = O(1)$ such that $(\delta' + k_T')/(\delta + \bar{k}_E^A) = \beta\mu'$, and, similarly, $b = O(1)$ such that $(\delta + \bar{k}_E^R)/(\delta + \bar{k}_E^A) = b\mu$. Then, μ' (μ) quantifies the relative speed between the rate of DNA demethylation (the repressive histone modification erasure rate) and the activating modification erasure rate. Furthermore, given that $(\delta + \bar{k}_E^R)/(k_M^A D_{tot}) = b\varepsilon\mu$, $(\delta' + k_T')/(k_M^A D_{tot}) = \beta\varepsilon\mu'$, $k_E^R/k_M^A = \mu\varepsilon'$ and $k_T'^*/k_M^A = \mu'\varepsilon'$, ε (ε') is a parameter that scales the ratio between the rate of basal (recruited) erasure and the auto-catalysis rate of each modification. Introducing the normalized time $\tau = t k_M^A D_{tot}$, the ODEs are

$$\begin{aligned}
\frac{d\bar{D}_1^R}{d\tau} &= (u_{10}^R + u_1^R + \alpha'(\bar{D}_2^R + \bar{D}_{12}^R))\bar{D} + \mu(b\varepsilon + \varepsilon'\bar{D}^A)\bar{D}_{12}^R \\
&\quad - (u_{20}^R + \alpha(\bar{D}_2^R + \bar{D}_{12}^R) + \bar{\alpha}(\bar{D}_1^R + \bar{D}_{12}^R))\bar{D}_1^R \\
&\quad - \mu'(\beta\varepsilon + \varepsilon'\bar{D}^A))\bar{D}_1^R \\
\frac{d\bar{D}_{12}^R}{d\tau} &= (u_{10}^R + \alpha'(\bar{D}_2^R + \bar{D}_{12}^R))\bar{D}_2^R \\
&\quad + (u_{20}^R + \alpha(\bar{D}_2^R + \bar{D}_{12}^R) + \bar{\alpha}(\bar{D}_1^R + \bar{D}_{12}^R))\bar{D}_1^R \\
&\quad - (\mu'(\beta\varepsilon + \varepsilon'\bar{D}^A) + \mu(b\varepsilon + \varepsilon'\bar{D}^A))\bar{D}_{12}^R \\
\frac{d\bar{D}_2^R}{d\tau} &= (u_{20}^R + u_2^R + \alpha(\bar{D}_2^R + \bar{D}_{12}^R) + \bar{\alpha}(\bar{D}_1^R + \bar{D}_{12}^R))\bar{D} \\
&\quad + \mu'(\beta\varepsilon + \varepsilon'\bar{D}^A)\bar{D}_{12}^R - (u_{10}^R + \alpha'(\bar{D}_2^R + \bar{D}_{12}^R))\bar{D}_2^R \\
&\quad - \mu(b\varepsilon + \varepsilon'\bar{D}^A))\bar{D}_2^R \\
\frac{d\bar{D}^A}{d\tau} &= (u_0^A + u^A + \bar{D}^A)\bar{D} \\
&\quad - (\varepsilon + \varepsilon'(\bar{D}_2^R + \bar{D}_{12}^R) + \varepsilon'(\bar{D}_1^R + \bar{D}_{12}^R))\bar{D}^A,
\end{aligned} \tag{3}$$

with $\bar{D} = 1 - \bar{D}_1^R - \bar{D}_{12}^R - \bar{D}_2^R - \bar{D}^A$ (see [11] for the complete derivation). It is important to point out that, in this model, if the gene expression is governed by a constitutive promoter, i.e., a promoter continuously active in standard conditions, without relying on external activators, then a constant non-basal *de-novo* establishment term for $\mathrm{D^A}$, u^A, must be considered.

A. Effect of epigenetic modifiers on model parameters

In order to determine how chromatin modifications alone (i.e., without permanent external inputs) affect gene expression memory, in our model we consider only epigenetic modifiers that are temporarily present in the system and study how their effect on chromatin state influences gene expression. From a biological point of view, one method to temporarily introduce epigenetic modifiers into the system is transient transfection. With this method, the concentration of epigenetic modifiers will gradually decrease due to dilution until it completely vanishes.

Now, starting with the establishment of H3K9me3, this aspect can be integrated into the model by writing the expression for the reaction rate constant of H3K9me3 establishment (k_W^2, see Table I), as $k_W^2 = \tilde{k}_W^2 W_2 e^{-\delta t}$. Here, W_2 is the total amount of the epigenetic modifier enhancing H3K9me3 establishment, such as KRAB [18], $\tilde{k}_W^2$ is a parameter independent of W_2, and δ denotes the dilution rate constant. The normalized input u_2^R in the ODEs (3) can then be written as

$$u_2^R = \frac{k_W^2}{k_M^A D_{tot}} = \frac{\tilde{k}_W^2}{k_M^A}\frac{W_2}{D_{tot}} e^{-\delta t \frac{k_M^A D_{tot}}{k_M^A D_{tot}}} = \tilde{u}_2^R \bar{W}_2 e^{-\varepsilon\tau}, \tag{4}$$

with $\tilde{u}_2^R = \tilde{k}_W^2/k_M^A$ and $\bar{W}_2 = W_2/D_{tot}$.

Similarly, the expression for the reaction rate constant of DNA methylation establishment (k_W^1, see Table I) can be written as $k_W^1 = \tilde{k}_W^1 W_1 e^{-\delta t}$. Here, W_1 is the total amount of DNMT3A, DNA methyltransferase that establishes *de novo* DNA methylation [1], and $\tilde{k}_W^1$ is a parameter independent of W_1. The normalized input u_1^R in the ODEs (3) can then be written as

$$u_1^R = \frac{k_W^1}{k_M^A D_{tot}} = \frac{\tilde{k}_W^1}{k_M^A}\frac{W_1}{D_{tot}} e^{-\delta t \frac{k_M^A D_{tot}}{k_M^A D_{tot}}} = \tilde{u}_1^R \bar{W}_1 e^{-\varepsilon\tau}, \tag{5}$$

with $\tilde{u}_1^R = \tilde{k}_W^1/k_M^A$ and $\bar{W}_1 = W_1/D_{tot}$.

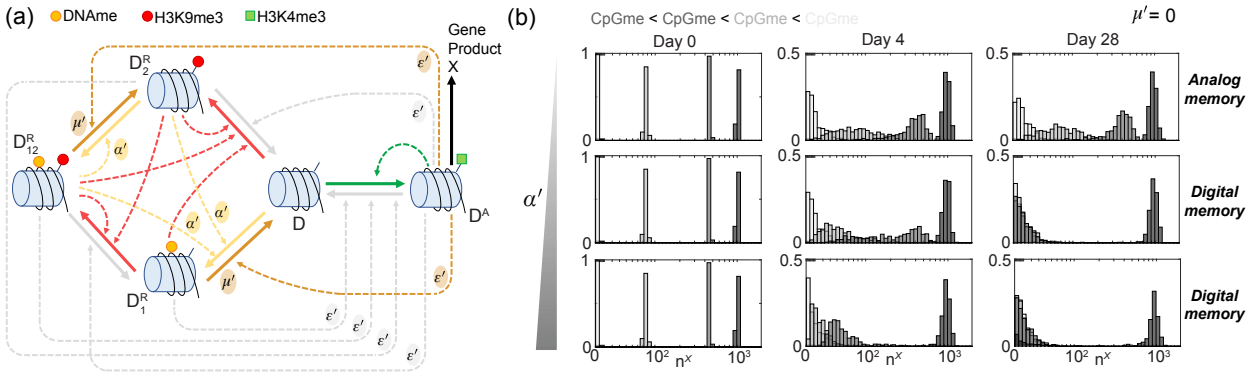

Fig. 1: Analog memory can be achieved when H3K9me3 does not catalyze DNA methylation (DNAme) establishment, i.e., when $\alpha' = 0$. (a) Diagram of complete chromatin modification circuit. The species are unmodified nucleosome (D), nucleosome with H3K4me3 ($\mathrm{D^A}$), nucleosome with DNAme ($\mathrm{D_1^R}$), nucleosome with H3K9me3 ($\mathrm{D_2^R}$), and nucleosome with both H3K9me3 and DNAme ($\mathrm{D_{12}^R}$). Here, solid arrows denote the nucleosome modification processes and gene expression, while dashed arrows denote the enzyme recruitment processes. We use red for processes involved in the establishment of H3K9me3, light (dark) orange for processes involved in the establishment (demethylation) of DNAme, green for processes involved in the establishment of H3K4me3, gray for processes involved in the erasure of histone modifications, and black for gene expression. **(b)** Probability distributions of the system represented by reactions in Tables I, II for different values of α'. The distributions are obtained computationally using SSA [10] and we denote the gene expression level as n^X (logicle scale). The parameter values used for these simulations are listed in Section VI-C. In particular, we consider $\alpha' = 0, 0.1$ and four initial conditions, that are (n_{12}^R,n_1^R,n_2^R,n^A): (14,0,1,0), (6,0,8,1), (4,0,5,6), and (1,0,1,13), going from light to dark gray, respectively. For all the simulations, we set $\mu' = 0$, $\alpha = \bar{\alpha} = 1$, $\varepsilon = 0.08$, $\varepsilon' = 25$, $\mu = 0.1$, $b = \beta = 1$, and $\mathrm{D_{tot}} = 15$ Finally, to realize each distribution, we conduct $N = 1000$ simulations.

Finally, the expression for the reaction rate constants of DNA demethylation processes (k_T' and $k_T'^*$, see Table I) can be written as $k_T' = k_{T1}' + \tilde{k}_T' T e^{-\delta t}$ and $k_T'^* = k_{T1}'^* + \tilde{k}_T'^* T e^{-\delta t}$. Here, T is the total amount of the transiently transfected modifier that catalyzes DNA demethylation, such as TET1 [3], [16], [19], k_{T1}' ($k_{T1}'^*$) is the component of the rate coefficient that does not depend on the external TET1 transfected, and $\tilde{k}_T', \tilde{k}_T'^*$ are parameters independent of T. The parameter μ' in the ODEs (3) can then be written as

$$\mu' = \frac{k_T'^*}{k_E^A} = \frac{k_{T1}'^*}{k_E^A} + \frac{\tilde{k}_T'^* D_{tot}}{k_E^A} \frac{T}{D_{tot}} e^{-\delta \frac{k_M^A D_{tot}}{k_M^A D_{tot}}} = \mu_1' + \tilde{\mu}' \bar{T} e^{-\varepsilon\tau}, \quad (6)$$

with $\mu_1' = \frac{k_{T1}'^*}{k_E^A}$, $\tilde{\mu}'$, and $\bar{T} = T/D_{tot}$.

III. Gene expression model

During gene expression, DNA is first transcribed into mRNA m (transcription) and then mRNA is translated into the gene product X (translation). Chromatin modifications, by regulating DNA compaction, affect transcription and then gene expression [1], [20]. Therefore, we assume that transcription is predominantly allowed by $\mathrm{D^A}$, while allowing a low level of transcription to all the other species. Additionally, m decay depends on dilution, due to cell division, and degradation, while X decay depends only on dilution [21] (see reactions in Table II). Introducing the normalized time $\tau = tk_M^A D_{tot}$ and the non-dimensional parameters $\bar{\beta}_m^A = \beta_m^A / k_M^A D_{tot}$, $\bar{\beta}_m = \beta_m / k_M^A D_{tot}$, $\bar{\beta} = \beta / k_M^A D_{tot}$, $\bar{\gamma}_m = \gamma_m / k_M^A D_{tot}$, $\bar{\delta} = \delta / k_M^A D_{tot}$, the gene expression ODE model can be written as

$$\frac{d\bar{m}}{d\tau} = \bar{\beta}_m^A \bar{D}^A + \bar{\beta}_m (\bar{D} + \bar{D}_1^R + \bar{D}_2^R + \bar{D}_{12}^R) - \bar{\gamma}_m \bar{m},$$
$$\frac{d\bar{X}}{d\tau} = \bar{\beta}\bar{m} - \bar{\delta}\bar{X}. \quad (7)$$

IV. Impact of α' on the system's behavior

We start our analysis by studying the stochastic behavior of the full model, i.e., model combining the complete chromatin modification circuit model with the gene expression model, with the aim of understanding the impact of α' (normalized rate of DNA methylation (DNAme) establishment catalyzed by H3K9me3) on the gene expression level probability distribution and, therefore, on the nature of gene expression memory achievable.

In particular, let us consider the parameter regime in which $\mu' = 0$, i.e., the DNA demethylation rate can be considered as approximately zero compared to histone modification erasure rate. This is because, without external epigenetic modifiers, it has been shown that the (passive) DNA demethylation process is significantly slow [8], [22]. When $\mu' = 0$, analog memory can be achieved only when $\alpha' = 0$, that is, when H3K9me3 does not recruit DNAme writers (Fig. 1(b)). For $\alpha' > 0$, the gene expression level shifts either to a low or a

high level. Furthermore, the higher α', the more the distribution tends to shift towards a low gene expression level (Fig. 1(b)).

Overall, these results suggest we can have analog memory only when DNA demethylation rate is sufficiently small compared to histone modification dynamics (that is, $\mu' \approx 0$) and H3K9me3 does not catalyze DNAme establishment ($\alpha' = 0$).

A. Reduced 2D chromatin modification circuit model

When these parameter conditions are verified and external epigenetic modifiers are not introduced into the system, then the total number of nucleosomes with DNAme remains constant. Denoting the fraction of nucleosomes with DNAme in the gene of interest as $\bar{Y}_1 = \bar{D}_1^R + \bar{D}_{12}^R$, the dynamics of the original model (3) can then be described by a reduced 2D ODE model. Before deriving the reduced model, let us first merge into a unique rate the rates associated with the catalysis of H3K9me3 establishment by $\bar{D}_{12}^R$ and assume that this is equal to the rate of H3K9me3 establishment by $\bar{D}_1^R$. Similarly, let us merge the rates associated with the erasure of H3K4me3 by $\bar{D}_{12}^R$ and assume that this rate is equal to the erasure rate of H3K4me3 by $\bar{D}_1^R$. These simplifying assumptions do not affect the qualitative results related to the effect of the cooperative and competitive interactions among chromatin modifications on epigenetic cell memory. The ODE model (3) can then be rewritten as

$$\begin{aligned}
\frac{d\bar{D}_1^R}{d\tau} &= (u_{10}^R + u_1^R + \alpha'(\bar{D}_2^R + \bar{D}_{12}^R))\bar{D} + \mu(b\varepsilon + \varepsilon'\bar{D}^A)\bar{D}_{12}^R \\
&\quad - (u_{20}^R + \alpha(\bar{D}_2^R + \bar{D}_{12}^R) + \bar{\alpha}(\bar{D}_1^R + \bar{D}_{12}^R))\bar{D}_1^R \\
&\quad - \mu'(\beta\varepsilon + \varepsilon'\bar{D}^A))\bar{D}_1^R \\
\frac{d\bar{D}_{12}^R}{d\tau} &= (u_{10}^R + \alpha'(\bar{D}_2^R + \bar{D}_{12}^R))\bar{D}_2^R \\
&\quad + (u_{20}^R + \alpha\bar{D}_2^R + \bar{\alpha}(\bar{D}_1^R + \bar{D}_{12}^R))\bar{D}_1^R \\
&\quad - (\mu'(\beta\varepsilon + \varepsilon'\bar{D}^A) + \mu(b\varepsilon + \varepsilon'\bar{D}^A))\bar{D}_{12}^R \qquad (8) \\
\frac{d\bar{D}_2^R}{d\tau} &= (u_{20}^R + u_2^R + \alpha\bar{D}_2^R + \bar{\alpha}(\bar{D}_1^R + \bar{D}_{12}^R))\bar{D} \\
&\quad + \mu'(\beta\varepsilon + \varepsilon'\bar{D}^A)\bar{D}_{12}^R - (u_{10}^R + \alpha'(\bar{D}_2^R + \bar{D}_{12}^R))\bar{D}_2^R \\
&\quad - \mu(b\varepsilon + \varepsilon'\bar{D}^A))\bar{D}_2^R \\
\frac{d\bar{D}^A}{d\tau} &= (u_0^A + u^A + \bar{D}^A)\bar{D} \\
&\quad - (\varepsilon + \varepsilon'(\bar{D}_2^R) + \varepsilon'(\bar{D}_1^R + \bar{D}_{12}^R))\bar{D}^A,
\end{aligned}$$

Now, let us introduce the following proposition:

Proposition IV.1. *Let $\alpha' = c\mu_1'$, with $c = O(1)$, and let us consider the following system, shown in Fig. 2(a):*

$$\begin{aligned}
\frac{d\bar{D}_2^R}{d\tau} &= (\alpha\bar{D}_2^R + \bar{\alpha}\bar{Y}_1)\bar{D} - \mu(b\varepsilon + \varepsilon'\bar{D}^A)\bar{D}_2^R, \qquad (9) \\
\frac{d\bar{D}^A}{d\tau} &= (u^A + \bar{D}^A)\bar{D} - (\varepsilon + \varepsilon'(\bar{D}_2^R + \bar{Y}_1))\bar{D}^A,
\end{aligned}$$

with $\bar{D} = 1 - \bar{D}^A - \bar{D}_2^R - \bar{Y}_1$ and $\bar{Y}_1 = constant$. Then, for sufficiently small μ_1' and $\alpha' = c\mu_1'$, any $(\bar{D}_2^R(\tau, \mu_1'), \bar{D}^A(\tau, \mu_1'))$ from the solution of (8) can be expressed with the following expansions:

$$\begin{aligned}
\bar{D}_2^R(\tau, \mu_1') &= \bar{D}_2^{R^*}(\tau) + O(\mu_1'), \\
\bar{D}^A(\tau, \mu_1') &= \bar{D}^{A*}(\tau) + O(\mu_1'), \qquad (10)
\end{aligned}$$

in which $(\bar{D}_2^{R^*}(\tau), \bar{D}^{A*}(\tau))$ is the solution of (9) and with the error estimate holding as $\mu_1' \to 0$ uniformly for $0 \leq \tau \leq T$.

Proof. Let us start by assuming negligible basal *de novo* establishment ($u_{10}^R = u_{20}^R = u_0^A = 0$) and introducing the variable $\bar{Y}_1 = \bar{D}_1^R + \bar{D}_{12}^R$. System (8) can then be rewritten as

$$\begin{aligned}
\frac{d\bar{Y}_1}{d\tau} &= (u_1^R)\bar{D} + (\alpha'(\bar{D}_2^R + \bar{D}_{12}^R))(\bar{D} + \bar{D}_2^R) \\
&\quad - \mu'(\beta\varepsilon + \varepsilon'\bar{D}^A)\bar{Y}_1 \\
\frac{d\bar{D}_{12}^R}{d\tau} &= (\alpha'(\bar{D}_2^R + \bar{D}_{12}^R))\bar{D}_2^R + (\alpha\bar{D}_2^R + \bar{\alpha}\bar{Y}_1)\bar{D}_1^R \\
&\quad - (\mu'(\beta\varepsilon + \varepsilon'\bar{D}^A) + \mu(b\varepsilon + \varepsilon'\bar{D}^A))\bar{D}_{12}^R \qquad (11) \\
\frac{d\bar{D}_2^R}{d\tau} &= (u_2^R + \alpha\bar{D}_2^R + \bar{\alpha}\bar{Y}_1)\bar{D} + \mu'(\beta\varepsilon + \varepsilon'\bar{D}^A)\bar{D}_{12}^R \\
&\quad - (\alpha'(\bar{D}_2^R + \bar{D}_{12}^R))\bar{D}_2^R - (\mu(b\varepsilon + \varepsilon'\bar{D}^A))\bar{D}_2^R \\
\frac{d\bar{D}^A}{d\tau} &= (u^A + \bar{D}^A)\bar{D} - (\varepsilon + \varepsilon'\bar{D}_2^R + \varepsilon'\bar{Y}_1)\bar{D}^A,
\end{aligned}$$

in which $\bar{D} = 1 - \bar{Y}_1 - \bar{D}_2^R - \bar{D}^A$ and $\bar{D}_1^R = \bar{Y}_1 - \bar{D}_{12}^R$. Now, let us introduce in (11) the expressions for u_2^R, u_1^R, and μ' derived in Section II-A (Exprs (4) - (6)):

$$\begin{aligned}
\frac{d\bar{Y}_1}{d\tau} &= \tilde{u}_1^R\bar{W}_1 e^{-\varepsilon\tau}\bar{D} + (\alpha'(\bar{D}_2^R + \bar{D}_{12}^R))(\bar{D} + \bar{D}_2^R) \\
&\quad - (\mu_1' + \tilde{\mu}'\bar{T}e^{-\varepsilon\tau})(\beta\varepsilon + \varepsilon'\bar{D}^A)\bar{Y}_1 \\
\frac{d\bar{D}_{12}^R}{d\tau} &= (\alpha'(\bar{D}_2^R + \bar{D}_{12}^R))\bar{D}_2^R + (\alpha\bar{D}_2^R + \bar{\alpha}\bar{Y}_1)\bar{D}_1^R \\
&\quad - ((\mu_1' + \tilde{\mu}'\bar{T}e^{-\varepsilon\tau})(\beta\varepsilon + \varepsilon'\bar{D}^A))\bar{D}_{12}^R \\
&\quad - \mu(b\varepsilon + \varepsilon'\bar{D}^A)\bar{D}_{12}^R \qquad (12) \\
\frac{d\bar{D}_2^R}{d\tau} &= (\tilde{u}_2^R\bar{W}_2 e^{-\varepsilon\tau} + \alpha\bar{D}_2^R + \bar{\alpha}\bar{Y}_1)\bar{D} \\
&\quad + (\mu_1' + \tilde{\mu}'\bar{T}e^{-\varepsilon\tau})(\beta\varepsilon + \varepsilon'\bar{D}^A)\bar{D}_{12}^R \\
&\quad - (\alpha'(\bar{D}_2^R + \bar{D}_{12}^R) + \mu(b\varepsilon + \varepsilon'\bar{D}^A))\bar{D}_2^R \\
\frac{d\bar{D}^A}{d\tau} &= (u^A + \bar{D}^A)\bar{D} - (\varepsilon + \varepsilon'\bar{D}_2^R + \varepsilon'\bar{Y}_1)\bar{D}^A.
\end{aligned}$$

After a temporary phase, during which the external inputs gradually decrease until they completely vanish ($e^{-\varepsilon\tau} \approx 0$), system (12) can then be rewritten as

$$\begin{aligned}
\frac{d\bar{Y}_1}{d\tau} &= \alpha'(\bar{D}_2^R + \bar{D}_{12}^R)(\bar{D} + \bar{D}_2^R) - \mu_1'(\beta\varepsilon + \varepsilon'\bar{D}^A)\bar{Y}_1 \\
\frac{d\bar{D}_{12}^R}{d\tau} &= (\alpha'(\bar{D}_2^R + \bar{D}_{12}^R))\bar{D}_2^R + (\alpha\bar{D}_2^R + \bar{\alpha}\bar{Y}_1)\bar{D}_1^R
\end{aligned}$$

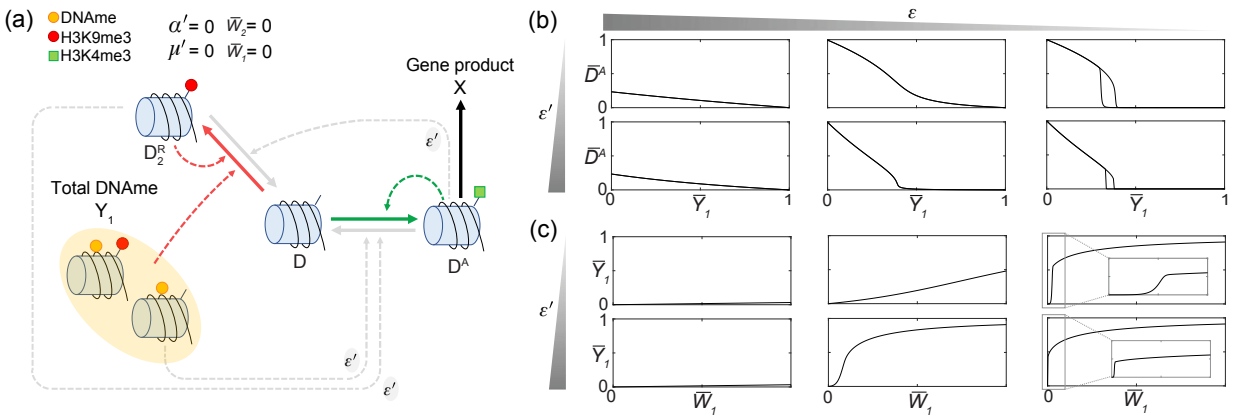

Fig. 2: Impact of ε and ε' on the response between H3K4me3 ($\bar{D}^A$), DNA methylation grade ($\bar{Y}_1$) at the gene, and initial level of DNA methylation writer DNMT3A ($\bar{W}_1$). (a) Simplified chromatin modification circuit diagram obtained when $\alpha' = 0$, $\mu' = 0$, $\bar{W}_1 = 0$), and $\bar{W}_2 = 0$. **(b)** Dose-response curve for $(\bar{Y}_1, \bar{D}^A)$ for different values of ε and ε', obtained from simulations of system (9) with $(\bar{Y}_1, \bar{D}_2^R, \bar{D}^A) = (j, 0, 1-j)$ as initial conditions, with $0 \leq j \leq 1$. **(c)** Dose-response curve for $(\bar{W}_1, \bar{Y}_1)$, for different values of ε and ε' obtained from simulations of system (9) with $(\bar{Y}_1, \bar{D}_2^R, \bar{D}^A) = (0, 0, 1)$ as initial condition and $\bar{W}_1 = [0, 4]$. For panels (b) and (c), we consider $\varepsilon = 0.0001, 0.1, 50$ and $\varepsilon' = 1, 25$. The other parameter values are $\beta = 1$, $\tilde{u}_1^R = 1$, $\alpha = \bar{\alpha} = 1$, $\mu = 0.1$, $b = 1$, $u^A = 15$. Here, the external input dynamics is modeled as a pulse that exponentially decreases over time and $\bar{W}_1$ corresponds to the external input value at time 0. In our model, α' is the normalized rate of DNAme establishment catalyzed by H3K9me3, μ' quantifies the relative speed between the rate of DNA demethylation and the activating modification erasure rate, and ε (ε') is the parameter scaling the rate of the basal erasure process (recruited erasure process) with respect to the auto-catalysis rate of each chromatin mark.

$$
\begin{aligned}
&- (\mu_1'(\beta\varepsilon + \varepsilon'\bar{D}^A) + \mu(b\varepsilon + \varepsilon'\bar{D}^A))\bar{D}_{12}^R \quad (13)\\
\frac{d\bar{D}_2^R}{d\tau} &= (\alpha\bar{D}_2^R + \bar{\alpha}\bar{Y}_1)\bar{D} + \mu_1'(\beta\varepsilon + \varepsilon'\bar{D}^A)\bar{D}_{12}^R\\
&- (\alpha'(\bar{D}_2^R + \bar{D}_{12}^R) + \mu(b\varepsilon + \varepsilon'\bar{D}^A))\bar{D}_2^R\\
\frac{d\bar{D}^A}{d\tau} &= (u^A + \bar{D}^A)\bar{D} - (\varepsilon + \varepsilon'\bar{D}_2^R + \varepsilon'\bar{Y}_1)\bar{D}^A.
\end{aligned}
$$

Now, let us set $\mu_1' = 0$ (and then $\alpha' = c\mu_1' = 0$), obtaining

$$
\begin{aligned}
\frac{d\bar{Y}_1}{d\tau} &= 0\\
\frac{d\bar{D}_{12}^R}{d\tau} &= (\alpha\bar{D}_2^R + \bar{\alpha}\bar{Y}_1)\bar{D}_1^R - \mu(b\varepsilon + \varepsilon'\bar{D}^A)\bar{D}_{12}^R \quad (14)\\
\frac{d\bar{D}_2^R}{d\tau} &= (\alpha\bar{D}_2^R + \bar{\alpha}\bar{Y}_1)\bar{D} - (\mu(b\varepsilon + \varepsilon'\bar{D}^A))\bar{D}_2^R\\
\frac{d\bar{D}^A}{d\tau} &= (u^A + \bar{D}^A)\bar{D} - (\varepsilon + \varepsilon'\bar{D}_2^R + \varepsilon'\bar{Y}_1)\bar{D}^A,
\end{aligned}
$$

in which $\bar{D} = 1 - \bar{Y}_1 - \bar{D}_2^R - \bar{D}^A$ and $\bar{D}_1^R = \bar{Y}_1 - \bar{D}_{12}^R$. From (14), it follows that $\bar{Y}_1 = constant$. This implies that, during the transient phase in which external inputs are introduced into the system, $\bar{Y}_1$ evolves according to $d\bar{Y}_1/d\tau = \tilde{u}_1^R\bar{W}_1 e^{-\varepsilon\tau}\bar{D}$ until $e^{-\varepsilon\tau} \approx 0$, at which point $\bar{Y}_1$ reaches a certain value. Now, let us define $x = (\bar{Y}_1, \bar{D}_{12}^R, \bar{D}_2^R, \bar{D}^A)$, and denote as $f(x, \mu_1')$ ($f(x, 0)$) the matrix in which each row corresponds to the right-hand side of each equation in (13) (in (14)). Then, it is evident that $f(x, \mu_1')$ and $f(x, 0)$ are smooth functions of their variables. Furthermore, since each entry of $\partial f(x, 0)/\partial x$ is bounded for any x, we have that $||\partial f(x, 0)/\partial x||_2 < L$, with $L > 0$ being a real number. From this, it follows that there exists a unique solution $x_0(\tau)$ for the system (14) on the interval $0 \leq \tau \leq T$ (Existence-Uniqueness Theorem, [23]). We can then conclude that system (13) is regularly perturbed, with small parameter μ_1', and its solution can be expressed as a Taylor expansion $x(\tau, \mu_1') = x_0(\tau) + O(\mu_1')$ [24]. In particular, since the last two ODEs in (14) depend only on $\bar{D}_2^R$, $\bar{D}^A$, and $\bar{Y}_1$, once the external inputs die out ($e^{-\varepsilon\tau} \approx 0$), $\bar{Y}_1$ remains constant and the dynamics of ($\bar{D}^A$, $\bar{D}_2^R$) can be expressed as a series expansion as the one described in (10), in which $(\bar{D}_2^{R^*}(\tau), \bar{D}^{A*}(\tau))$ is the solution of the reduced 2D ODE model represented by the last two equations in (14), coinciding with the ODEs in (9). □

V. Impact of ε and ε' on the system's behavior

Let us now study the deterministic and stochastic behavior of our system, with the aim of understanding the impact of ε and ε' on the probability distribution of gene expression levels. As a reminder, ε and ε' are parameters scaling the rate of the basal erasure process and recruited erasure process, respectively, with respect to the auto-catalysis rate of each chromatin mark.

We start by studying the reduced 2D ODE model (Eqs (9)) in order to determine the effect of ε and ε' on the value of $\bar{D}^A$ at the equilibrium for different $\bar{Y}_1$, i.e., fractions of DNAme in the gene (Fig. 2(b)). For large values of ε, the system has a unique stable steady

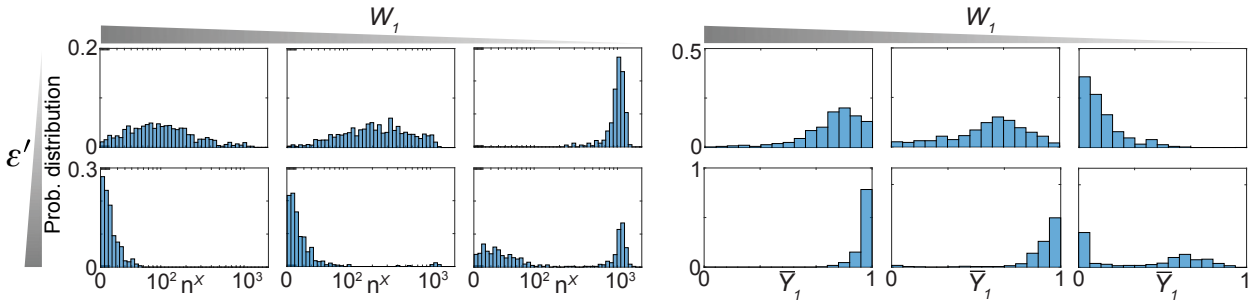

Fig. 3: The ultrasensitive response between the level of DNA methylation writer DNMT3A and DNA methylation grade leads to a bimodal distribution of gene expression levels. Probability distributions of the system represented by reactions in Tables I, II, after 28 days. We obtained them using SSA [10]. More precisely, on the left-hand side we have gene expression level probability distribution (logicle scale) and on the right-hand side we have the total DNAme level probability distributions. The parameter values used to generate these plots are listed in Section VI-C. In particular, we consider $\varepsilon = 0.13$, $\varepsilon' = 1.5, 25$ and $(n_{12}^R, n_1^R, n_2^R, n^A) = (0, 0, 0, \mathrm{D_{tot}})$ as initial condition. We consider $\mathrm{D_{tot}} = 15$, $N = 1000$ simulations to generate each distribution and, for each simulation conducted, the value of $\bar{W}_1$ was randomly selected from a uniformly distributed range, whose extremes are $\bar{W}_1 = [0, 0.4], [2.4, 2.8], [3.4, 3.8]$, respectively.

state characterized by low $\bar{D}^A$, with $\bar{D}^A$ decreasing as $\bar{Y}_1$ increases (Fig. 2(b)). As ε decreases, the value of D^A at steady-state increases, especially when $\bar{Y}_1$ is low, where $\bar{D}^A \approx 1$ (Fig. 2(b)). Reducing ε even further leads the system to be bistable for intermediate values of $\bar{Y}_1$ (Fig. 2(b)). Varying ε' does not significantly affect these trends, except when ε is small. In such cases, larger ε' leads to a smaller range of $\bar{Y}_1$ in which the system is bistable and to a smaller difference in the values of $\bar{D}^A$ between the two steady states (Fig. 2(b)). The second analysis aims to understand how ε and ε' affect the level of DNAme $\bar{Y}_1$ at equilibrium for various initial levels of $\bar{W}_1$, denoting DNAme writer DNMT3A (Fig. 2(c)). The analysis shows that larger values of $\bar{W}_1$ enable reaching higher values of $\bar{Y}_1$. Furthermore, when ε is low, high values of $\bar{Y}_1$ can be achieved, and, in case of small ε, higher ε' results in a more ultrasensitive curve (Fig. 2(c)).

Overall, these results suggest that high fractions of nucleosomes with H3K4me3, and consequently high levels of gene expression, are possible only for sufficiently small values of ε (Fig. 2(b)). In this parameter regime, when ε' is sufficiently high, $\bar{Y}_1$ shows an ultrasensitive response to transient dosage of DNAme writer DNMT3A. As a result, different ranges of values of initial DNMT3A transfection levels (W_1) would result only in either low or high gene expression levels (Fig. 2(b),(c)). To validate these results, we conduct a computational study on the full model, whose reactions are listed in Tables I, II (Fig. 3), using SSA [10]. For different ranges of initial DNMT3A levels (W_1), we obtain a bimodal probability distribution of gene expression levels when ε' is sufficiently large. For smaller values of ε', the stationary distribution shifts towards a unimodal shape, in agreement with our expectations derived from our deterministic analysis (Fig. 2(b),(c)).

VI. Concluding remarks and discussion

In this work, we investigate how chromatin modifications affect the memory of intermediate gene expression levels, in order to determine conditions under which the probability distributions of gene expression levels, observed in experiments and used to support digital memory, are also compatible with analog memory. To this end, we first introduce a mathematical model combining histone modifications and DNA methylation, derived starting from the one in [11] (Sections II, III). Our results show that, in the absence of external inputs (epigenetic modifiers), analog memory of gene expression can be achieved when H3K9me3 does not catalyze *de novo* DNA methylation, i.e., $\alpha' = 0$, and DNA methylation decay rate is negligible, i.e., $\mu' = 0$ (Section IV). When these critical conditions are not verified, our model predicts that only digital memory is achievable (Fig. 1(b)). We then conducted an additional deterministic analysis of a reduced version of the model, validated through a computational study of our full model. Our results show that, when considering a range of values uniformly distributed from which the external input value is randomly selected and assuming that the inputs decay over time then, in the parameter regime compatible with analog memory described above, the probability distributions of gene expression level are bimodal, resembling those obtained experimentally [8], only when ε is sufficiently small and ε' is sufficiently large.

Overall, our results suggest the key mechanisms determining when epigenetic cell memory is analog, highlighting the key role of DNA methylation. Experimental studies available in the literature confirm the low catalysis of DNA methylation by H3K9me3 ($\alpha' = 0$) in certain cell types [8]. Furthermore, previous

computational study suggests that long-term memory of silenced and active gene expression levels can be achieved only for sufficiently small values of ε [11], [25]. However, additional experiments are needed to validate all of our theoretical findings. For instance, chromosomally integrated, semi-synthetic genetic reporter system could be engineered in mammalian cells, and transient transfections of different epigenetic modifiers (such as DNMT3A, KRAB and TET1) could be performed. Then, our model and our theoretical results could help design key experiments to conduct, involving time-course flow cytometry measurements, coupled with bisulfite sequencing analysis at specific time points, in order to discern the nature of gene expression memory (analog or digital) and the contributions of DNA methylation and histone modifications to it.

APPENDIX

A. Chromatin modification circuit: reaction list

The reaction model describing the complete chromatin modification circuit can be written as in Table I.

B. Gene expression: reaction list

The reaction model associated with gene expression can be written as in Table II. In particular, defining the transcription rate constants as β_m^A and β_m, we assume $\beta_m < \beta_m^A$ (see Section III).

C. Parameter values used in the simulations

Simulations in Fig. 1: $k_{W0}^A = 0$, $k_W^A = 7.8075$ h^{-1}, $\bar{k}_E^A = 0.0118$ h^{-1}, $\delta = 0.0291$ h^{-1}, $\frac{k_M^A}{\Omega} = 0.0347$ h^{-1}, $\frac{k_E^A}{\Omega} = 0.8675$ h^{-1}, $k_{W0}^1 = 0$, $k_W^1 = 0$, $k_T' = 0$, $\delta' = 0$, $\frac{k_M'}{\Omega} = 0, 3.47 \cdot 10^{-4}, 3.47 \cdot 10^{-3}$ h^{-1}, $\frac{k_T'^*}{\Omega} = 0$, $k_{W0}^2 = 0$, $k_W^2 = 0$, $\bar{k}_E^R = 0.0012$ h^{-1}, $\frac{k_M}{\Omega} = 0.0347$ h^{-1}, $\frac{\bar{k}_M}{\Omega} = 0.0347$ h^{-1}, $\frac{k_E^R}{\Omega} = 0.0868$ h^{-1}, $\beta_m = 0.2556$ h^{-1}, $\beta_m^A = 0.0021$ h^{-1}, $\beta = 2.52$ h^{-1}, $\gamma_m = 0.24$ h^{-1}. *Simulations in Fig. 3*: $k_{W0}^A = 0$, $k_W^A = 7.8075$ h^{-1}, $\bar{k}_E^A = 0.0315$ h^{-1}, $\delta = 0.035$ h^{-1}, $\frac{k_M^A}{\Omega} = 0.0347$ h^{-1}, $\frac{k_E^A}{\Omega} = 0.0520, 0.8675$ h^{-1}, $k_{W0}^1 = 0$, $k_W^1 \in [0, 0.3643]e^{-\delta t}, [0.2602, 0.6246]e^{-\delta t}, [0.5205, 0.8848]e^{-\delta t}$ h^{-1}, $k_T' = 0$, $\delta' = 0$, $\frac{k_M'}{\Omega} = 0$, $\frac{k_T'^*}{\Omega} = 0$, $k_{W0}^2 = 0$, $k_W^2 = 0$, $\bar{k}_E^R = 0.0032$ h^{-1}, $\frac{k_M}{\Omega} = 0.0347$ h^{-1}, $\frac{\bar{k}_M}{\Omega} = 0.0347$ h^{-1}, $\frac{k_E^R}{\Omega} = 0.0052, 0.0868$ h^{-1}, $\beta_m = 0.2556$ h^{-1}, $\beta_m^A = 0.0021$ h^{-1}, $\beta = 2.52$ h^{-1}, $\gamma_m = 0.24$ h^{-1}. In the simulations of both figures, we set, as initial value for n^X of n^m, their steady states of the ODEs.

$\mathbf{R}_j$	**Reaction**	**Prop.Func.**(a_j)	**Param.**
1	$\mathrm{D} \xrightarrow{k_{W0}^A} \mathrm{D^A}$	$a_1 = k_{W0}^A n^D$	k_{W0}^A
2	$\mathrm{D} \xrightarrow{k_W^A} \mathrm{D^A}$	$a_2 = k_W^A n^D$	k_W^A
3	$\mathrm{D^A} \xrightarrow{\bar{k}_E^A} \mathrm{D}$	$a_3 = \bar{k}_E^A n^A$	$\bar{k}_E^A$
4	$\mathrm{D^A} \xrightarrow{\delta} \mathrm{D}$	$a_4 = \delta n^A$	δ
5	$\mathrm{D} + \mathrm{D^A} \xrightarrow{k_M^A} \mathrm{D^A} + \mathrm{D^A}$	$a_5 = \frac{k_M^A}{\Omega} n^D n^A$	$\frac{k_M^A}{\Omega}$
6	$\mathrm{D^A} + \mathrm{D_1^R} \xrightarrow{k_E^A} \mathrm{D} + \mathrm{D_1^R}$	$a_6 = \frac{k_E^A}{\Omega} n^A n_1^R$	$\frac{k_E^A}{\Omega}$
7	$\mathrm{D^A} + \mathrm{D_{12}^R} \xrightarrow{k_E^A} \mathrm{D} + \mathrm{D_{12}^R}$	$a_7 = \frac{k_E^A}{\Omega} n^A n_{12}^R$	$\frac{k_E^A}{\Omega}$
8	$\mathrm{D^A} + \mathrm{D_2^R} \xrightarrow{k_E^A} \mathrm{D} + \mathrm{D_2^R}$	$a_8 = \frac{k_E^A}{\Omega} n^A n_2^R$	$\frac{k_E^A}{\Omega}$
9	$\mathrm{D^A} + \mathrm{D_{12}^R} \xrightarrow{k_E^A} \mathrm{D} + \mathrm{D_{12}^R}$	$a_9 = \frac{k_E^A}{\Omega} n^A n_{12}^R$	$\frac{k_E^A}{\Omega}$
10	$\mathrm{D} \xrightarrow{k_{W0}^1} \mathrm{D_1^R}$	$a_{10} = k_{W0}^1 n^D$	k_{W0}^1
11	$\mathrm{D} \xrightarrow{k_W^1} \mathrm{D_1^R}$	$a_{11} = k_W^1 n^D$	k_W^1
12	$\mathrm{D_1^R} \xrightarrow{k_T'} \mathrm{D}$	$a_{12} = k_T' n_1^R$	k_T'
13	$\mathrm{D_1^R} \xrightarrow{\delta'} \mathrm{D}$	$a_{13} = \delta' n_1^R$	δ'
14	$\mathrm{D} + \mathrm{D_2^R} \xrightarrow{k_M'} \mathrm{D_1^R} + \mathrm{D_2^R}$	$a_{14} = \frac{k_M'}{\Omega} n^D n_2^R$	$\frac{k_M'}{\Omega}$
15	$\mathrm{D} + \mathrm{D_{12}^R} \xrightarrow{k_M'} \mathrm{D_1^R} + \mathrm{D_{12}^R}$	$a_{15} = \frac{k_M'}{\Omega} n^D n_{12}^R$	$\frac{k_M'}{\Omega}$
16	$\mathrm{D_1^R} + \mathrm{D^A} \xrightarrow{k_T'^*} \mathrm{D} + \mathrm{D^A}$	$a_{16} = \frac{k_T'^*}{\Omega} n_1^R n^A$	$\frac{k_T'^*}{\Omega}$
17	$\mathrm{D} \xrightarrow{k_{W0}^2} \mathrm{D_2^R}$	$a_{17} = k_{W0}^2 n^D$	k_{W0}^2
18	$\mathrm{D} \xrightarrow{k_W^2} \mathrm{D_2^R}$	$a_{18} = k_W^2 n^D$	k_W^2
19	$\mathrm{D_2^R} \xrightarrow{\bar{k}_E^R} \mathrm{D}$	$a_{19} = \bar{k}_E^R n_2^R$	$\bar{k}_E^R$
20	$\mathrm{D_2^R} \xrightarrow{\delta} \mathrm{D}$	$a_{20} = \delta n_2^R$	δ
21	$\mathrm{D} + \mathrm{D_2^R} \xrightarrow{k_M} \mathrm{D_2^R} + \mathrm{D_2^R}$	$a_{21} = \frac{k_M}{\Omega} n^D n_2^R$	$\frac{k_M}{\Omega}$
22	$\mathrm{D} + \mathrm{D_{12}^R} \xrightarrow{k_M} \mathrm{D_2^R} + \mathrm{D_{12}^R}$	$a_{22} = \frac{k_M}{\Omega} n^D n_{12}^R$	$\frac{k_M}{\Omega}$
23	$\mathrm{D} + \mathrm{D_1^R} \xrightarrow{\bar{k}_M} \mathrm{D_2^R} + \mathrm{D_1^R}$	$a_{23} = \frac{\bar{k}_M}{\Omega} n^D n_1^R$	$\frac{\bar{k}_M}{\Omega}$
24	$\mathrm{D} + \mathrm{D_{12}^R} \xrightarrow{\bar{k}_M} \mathrm{D_2^R} + \mathrm{D_{12}^R}$	$a_{24} = \frac{\bar{k}_M}{\Omega} n^D n_{12}^R$	$\frac{\bar{k}_M}{\Omega}$
25	$\mathrm{D_2^R} + \mathrm{D^A} \xrightarrow{k_E^R} \mathrm{D} + \mathrm{D^A}$	$a_{25} = \frac{k_E^R}{\Omega} n_2^R n^A$	$\frac{k_E^R}{\Omega}$
26	$\mathrm{D_1^R} \xrightarrow{k_{W0}^2} \mathrm{D_{12}^R}$	$a_{26} = k_{W0}^2 n_1^R$	k_{W0}^2
27	$\mathrm{D_{12}^R} \xrightarrow{\bar{k}_E^R} \mathrm{D_1^R}$	$a_{27} = \bar{k}_E^R n_{12}^R$	$\bar{k}_E^R$
28	$\mathrm{D_{12}^R} \xrightarrow{\delta} \mathrm{D_1^R}$	$a_{28} = \delta n_{12}^R$	δ
29	$\mathrm{D_1^R} + \mathrm{D_2^R} \xrightarrow{k_M} \mathrm{D_{12}^R} + \mathrm{D_2^R}$	$a_{29} = \frac{k_M}{\Omega} n_1^R n_2^R$	$\frac{k_M}{\Omega}$
30	$\mathrm{D_1^R} + \mathrm{D_{12}^R} \xrightarrow{k_M} \mathrm{D_{12}^R} + \mathrm{D_{12}^R}$	$a_{30} = \frac{k_M}{\Omega} n_1^R n_{12}^R$	$\frac{k_M}{\Omega}$
31	$\mathrm{D_1^R} + \mathrm{D_1^R} \xrightarrow{\bar{k}_M} \mathrm{D_{12}^R} + \mathrm{D_1^R}$	$a_{31} = \frac{\bar{k}_M}{\Omega} \frac{n_1^R(n_1^R-1)}{2}$	$\frac{\bar{k}_M}{\Omega}$
32	$\mathrm{D_1^R} + \mathrm{D_{12}^R} \xrightarrow{\bar{k}_M} \mathrm{D_{12}^R} + \mathrm{D_{12}^R}$	$a_{32} = \frac{\bar{k}_M}{\Omega} n_1^R n_{12}^R$	$\frac{\bar{k}_M}{\Omega}$
33	$\mathrm{D_{12}^R} + \mathrm{D^A} \xrightarrow{k_E^R} \mathrm{D_1^R} + \mathrm{D^A}$	$a_{33} = \frac{k_E^R}{\Omega} n_{12}^R n^A$	$\frac{k_E^R}{\Omega}$
34	$\mathrm{D_2^R} \xrightarrow{k_{W0}^1} \mathrm{D_{12}^R}$	$a_{34} = k_{W0}^1 n_2^R$	k_{W0}^1
35	$\mathrm{D_{12}^R} \xrightarrow{k_T'} \mathrm{D_2^R}$	$a_{35} = k_T' n_{12}^R$	k_T'
36	$\mathrm{D_{12}^R} \xrightarrow{\delta'} \mathrm{D_2^R}$	$a_{36} = \delta' n_{12}^R$	δ'
37	$\mathrm{D_2^R} + \mathrm{D_2^R} \xrightarrow{k_M'} \mathrm{D_{12}^R} + \mathrm{D_2^R}$	$a_{37} = \frac{k_M'}{\Omega} \frac{n_2^R(n_2^R-1)}{2}$	$\frac{k_M'}{\Omega}$
38	$\mathrm{D_2^R} + \mathrm{D_{12}^R} \xrightarrow{k_M'} \mathrm{D_{12}^R} + \mathrm{D_{12}^R}$	$a_{38} = \frac{k_M'}{\Omega} n_2^R n_{12}^R$	$\frac{k_M'}{\Omega}$
39	$\mathrm{D_{12}^R} + \mathrm{D^A} \xrightarrow{k_T'^*} \mathrm{D_2^R} + \mathrm{D^A}$	$a_{39} = \frac{k_T'^*}{\Omega} n_{12}^R n^A$	$\frac{k_T'^*}{\Omega}$

TABLE I: Full chromatin modification circuit model: reactions

REFERENCES

[1] C. D. Allis, M.-L. Caparros, T. Jenuwein, and D. Reinberg, *Epigenetics*. Cold Spring Harbor Laboratory Press, Second Edition, 2015.

[2] N. Carey, *The epigenetic revolution*. Columbia University Press, 2013.

[3] S. Huang, M. Litt, and C. A. Blakey, *Epigenetic Gene Expression and Regulation*. Academic Press, 2015.

[4] E. Li and Y. Zhang, "Dna methylation in mammals," *Cold Spring Harb Perspect Biol*, vol. 6, no. 5, 2014.

[5] A. P. Bird and M. H. Taggart, "Variable patterns of total dna and

$\mathbf{R}_j$	**Reaction**	**Prop.Func.**(a_j)	**Param.**
1	$\mathrm{D^A} \xrightarrow{\beta_m^A} \mathrm{D^A + m}$	$a_1 = \beta_m^A n^A$	β_m^A
2	$\mathrm{D} \xrightarrow{\beta_m} \mathrm{D + m}$	$a_2 = \beta_m n^D$	β_m
3	$\mathrm{D_1^R} \xrightarrow{\beta_m} \mathrm{D_1^R + m}$	$a_3 = \beta_m n_1^R$	β_m
4	$\mathrm{D_2^R} \xrightarrow{\beta_m} \mathrm{D_2^R + m}$	$a_4 = \beta_m n_2^R$	β_m
5	$\mathrm{D_{12}^R} \xrightarrow{\beta_m} \mathrm{D_{12}^R + m}$	$a_5 = \beta_m n_{12}^R$	β_m
6	$\mathrm{m} \xrightarrow{\beta} \mathrm{m + X}$	$a_6 = \beta n^m$	β
7	$\mathrm{m} \xrightarrow{\gamma_m} \emptyset$	$a_7 = \gamma_m n^m$	γ_m
8	$\mathrm{X} \xrightarrow{\delta} \emptyset$	$a_8 = \delta n^X$	δ

TABLE II: Gene expression model: reactions

rdna methylation in animals," *Nucleic Acids Res*, vol. 8, no. 7, pp. 1485–1497, 1980.

[6] E. Hodges, A. Molaro, C. O. Dos Santos, P. Thekkat, Q. Song, P. J. Uren, J. Park, J. Butler, S. Rafii, W. R. McCombie, A. D. Smith, and G. J. Hannon, "Dna methylation changes and complex intermediate states accompany lineage specificity in the adult hematopoietic compartment," *Molecular cell*, vol. 44, no. 1, pp. 17–28, 2011.

[7] M. B. Stadler, R. Murr, L. Burger, R. Ivanek, F. Lienert, A. Schöler, E. van Nimwegen, C. Wirbelauer, E. J. Oakeley, D. Gaidatzis, T. V. Tiwari, and D. Schübeler, "Dna-binding factors shape the mouse methylome at distal regulatory regions," *Nature*, vol. 480, no. 7378, pp. 490–495, 2011.

[8] L. Bintu, J. Yong, Y. E. Antebi, K. McCue, Y. Kazuki, N. Uno, M. Oshimura, and M. B. Elowitz, "Dynamics of epigenetic regulation at the single-cell level," *Science*, 2016.

[9] Z. Yao, C. T. J. van Velthoven, T. N. Nguyen, J. Goldy, A. E. Sedeno-Cortes, F. Baftizadeh, D. Bertagnolli, T. Casper, M. Chiang, K. Crichton, S.-L. Ding, O. Fong, E. Garren, A. Glandon, N. W. Gouwens, J. Gray, L. T. Graybuck, M. J. Hawrylycz, D. Hirschstein, M. Kroll, K. Lathia, C. Lee, B. Levi, D. McMillen, S. Mok, T. Pham, Q. Ren, C. Rimorin, N. Shapovalova, J. Sulc, S. M. Sunkin, M. Tieu, A. Torkelson, H. Tung, K. Ward, N. Dee, K. A. Smith, B. Tasic, and H. Zeng, "A taxonomy of transcriptomic cell types across the isocortex and hippocampal formation," *Cell*, vol. 184, no. 12, pp. 3222–3241, 2021.

[10] D. T. Gillespie, "Stochastic simulation of chemical kinetics," *Annual Review of Physical Chemistry*, vol. 58, no. 1, pp. 35–55, 2007.

[11] S. Bruno, R. J. Williams, and D. Del Vecchio, "Epigenetic cell memory: The gene's inner chromatin modification circuit," *PLOS Computational Biology*, vol. 18, no. 4, pp. 1 – 27, 2022.

[12] M. Trerotola, V. Relli, P. Simeone, and S. Alberti, "Epigenetic inheritance and the missing heritability," *Hum Genomics*, vol. 9, no. 1, p. 17, 2015.

[13] T. Zhang, S. Cooper, and N. Brockdorff, "The interplay of histone modifications - writers that read," *EMBO Rep*, vol. 16, no. 11, pp. 1467–1481, 2015.

[14] F. Fuks, P. J. Hurd, D. Wolf, X. Nan, A. P. Bird, and T. Kouzarides, "The methyl-cpg-binding protein mecp2 links dna methylation to histone methylation," *J Biol Chem*, vol. 278, no. 6, pp. 4035–4040, 2003.

[15] A. K. Upadhyay, J. R. Horton, X. Zhang, and X. Cheng, "Coordinated methyl-lysine erasure: structural and functional linkage of a jumonji demethylase domain and a reader domain," *Curr Opin Struct Biol*, vol. 21, no. 6, pp. 750–60, 2011.

[16] K. D. Rasmussen and K. Helin, "Role of tet enzymes in dna methylation, development, and cancer," *Genes Dev.*, vol. 30, no. 7, pp. 733–50, 2016.

[17] D. A. Brown, V. D. Cerbo, A. Feldmann, J. Ahn, S. Ito, N. P. Blackledge, M. Nakayama, M. McClellan, E. Dimitrova, A. H. Turberfield, H. K. Long, H. W. King, S. Kriaucionis, L. Schermelleh, T. G. Kutateladze, H. Koseki, and R. J. Klose, "The set1 complex selects actively transcribed target genes via multivalent interaction with cpg island chromatin," *Cell Rep*, vol. 20, no. 10, pp. 2313–2327, 2017.

[18] D. C. Schultz, K. Ayyanathan, D. Negorev, G. G. Maul, and F. J. Rauscher, "Setdb1: a novel kap-1-associated histone h3, lysine 9-specific methyltransferase that contributes to hp1-mediated silencing of euchromatic genes by krab zinc-finger proteins," *Annual Review of Physical Chemistry*, vol. 16, no. 8, pp. 919–32, 2002.

[19] C. Jin, Y. Lu, J. Jelinek, S. Liang, M. R. Estecio, M. C. Barton, and J.-P. J. Issa, "Tet1 is a maintenance dna demethylase that prevents methylation spreading in differentiated cells," *Nucleic Acids Research*, vol. 42, no. 11, pp. 6956–71, 2014.

[20] K. L. Huisinga, B. Brower-Toland, and S. C. Elgin, "The contradictory definitions of heterochromatin: transcription and silencing," *Chromosoma*, vol. 115, no. 2, pp. 110–22, 2006.

[21] D. Del Vecchio and R. M. Murray, *Biomolecular Feedback Systems*. Princeton University Press, 2014.

[22] M. Jackson, A. Krassowska, N. Gilbert, T. Chevassut, L. Forrester, J. Ansell, and B. Ramsahoye, "Severe global dna hypomethylation blocks differentiation and induces histone hyperacetylation in embryonic stem cells," *Mol Cell Biol*, vol. 24, no. 20, 2004.

[23] E. A. Coddington and N. Levinson, *Theory of Ordinary Differential Equations*. McGraw-Hill, 1955.

[24] F. C. Hoppensteadt, *Regular Perturbation Methods*, pp. 139–156. New York, NY: Springer New York, 1993.

[25] S. Bruno, R. J. Williams, and D. Del Vecchio, "Model reduction and stochastic analysis of the histone modification circuit," in *2022 European Control Conference (ECC)*, pp. 264–271, 2022.